ASSESSING BASEFLOW INDEX VULNERABILITY TO VARIATION IN DRY SPELL LENGTH FOR A RANGE OF CATCHMENT AND CLIMATE PROPERTIES

A. Longobardi [(1)*] and A. F. Van Loon [(2)]

[(1)] Department of Civil Engineering, University of Salerno, 84084 Fisciano (SA), Italy

[(2)] School of Geography, Earth and Environmental Sciences, University of Birmingham, B15 2TT, United Kingdom

*Corresponding author: Antonia Longobardi, Via Giovanni Paolo II, 132, 84084 Fisciano (SA), Italy. Tel. +39 089 963408; e-mail address: alongobardi@unisa.it

"This is a post-peer-review, pre-copyedit version of an article published in Hydrological Processes. The final authenticated version is available online at: https://doi.org/10.1002/hyp.13147"

Abstract

Baseflow index (BFI) prediction in ungauged basins has largely been based on the use of catchment physiographic attributes as dominant variables. In a context where changes in climate are increasingly evident, it is also important to study how the slow component of flow is potentially affected by climate. The aim of this study was to illustrate the impact of climate variability on the baseflow process based on analysis of daily rainfall characteristics and hydrological modelling simulation exercises validated with observed data. Ten catchments were analysed that span southern to northern Europe and range from arid Mediterranean to maritime temperate climate conditions. Additionally, more than two thousand virtual catchments were modelled that cover an extended gradient of physiographic and climate properties. The relative amounts of baseflow were summarized by the BFI. The catchment slow response delay time (Ks) was assumed to be a measure of catchment effects, and the impact of climate properties was investigated with the dry spell length (d). Well-drained and poorly-drained groups were identified based on Ks and d, and their response to an increase or decrease in dry spell length was analysed. Overall, for either well- or poorly-drained groups, an extension in dry spell length appeared to have minor effects on the baseflow compared with a decrease in dry spell length. Under the same dry spell variation, the BFI vulnerability appeared higher for catchments characterized by large initial d values in combination with poorly-drained systems, but attributing an equal weight to the variations in d both in the case of dry and wet initial conditions, it is in the end concluded that the BFI vulnerability appear higher for systems laying in the transition zone between well- and poorly-drained systems.

Keywords: Baseflow, Low flows, BFI, Dry spells, IAHCRES, catchment characteristics, climate

1. INTRODUCTION

The baseflow index (BFI), the ratio between the volume of baseflow and the volume of total streamflow, was originally recommended in the Low Flow Studies (Institute of Hydrology, 1980) for indexing the effect of geology on low flows; however, the BFI now represents a general index of catchment hydrological response. Among various applications, BFI has been implemented as an index of river flow regime classification (Kennard et al., 2010; Bejarano et al., 2010; Olden and Poff, 2012) and, as such, has also been used to detect hydrological regime changes along with other low flow indices (Sawicz et al., 2014, Coopersmith et al., 2014, Crooks and Kay, 2015).

Although the importance of the impact of geological catchment properties on BFI is universally understood (Gustard et al., 1989; Schneider et al., 2007; Longobardi and Villani, 2013; Zhang et al., 2013), the role of climate variables is less clear (Stoelzle et al., 2014; Van Loon and Laaha, 2015, Staudinger et al., 2015). Recent global scale assessments of BFI patterns and the relevant influence of various climate factors have generally focused on average climate characteristics, such as the mean annual precipitation, mean annual potential evapotranspiration, mean annual air temperature, and the intra-annual seasonality of precipitation (Beck et al., 2013; Sawicz et al., 2014).

A general agreement exists that climate (change or variability) has the potential to substantially alter river flow regimes. A global assessment has been reported in Arnell and Gosling, 2013. At the European scale, a large body of literature provides indications regarding the considerable climate change projections that will impact hydrological systems. As a general trend, high latitude areas of northern Europe appear to face an increase in the number of wet days and thus a decrease in the duration of dry spells. Conversely, southern Europe Mediterranean areas appear to face a decrease in the number of wet days and thus an increase in dry spell duration (Rajah et al., 2014; Jacob et al, 2014; Pascale et al., 2016). In a context where changes in climate are increasingly evident, it is important to study how the proportion of the slow component of flow is potentially affected by short-term rainfall properties.

The dry spell length and the catchment delay time, as well as their relative probability distributions, have in the past been considered to be primary descriptive parameters of the catchment hydrological response (Botter et al., 2013; Muller et al., 2014; Doulatyari et al., 2015). For example, Botter et al. (2013) showed how a combination of these descriptors can be used to determine the resilience of erratic and persistent regime systems to climate fluctuations. None of these studies, however, specifically focused on the baseflow component of the hydrograph. Therefore, in this study, we aim to illustrate the impact of climate variability and, in particular, the impact of dry spell duration on the baseflow process, summarized by the BFI index. We do this with a combined data-based and modelling study, investigating the hydrological behaviour of observed and virtual catchments that spanned a broad gradient of climate conditions and catchment properties.

In this study, two characteristic time scales were used, the dry spell length and the catchment delay time, to represent the effect of climate and catchment properties, respectively, on the BFI index. Investigated catchments were grouped into well-drained and poorly-drained systems based on their features. Catchments featured by perennial water resources, the well-drained group, were associated with prevailing slow streamflow components, large BFI values and long delays or recession times. Catchments with intermittent water resources, the poorly-drained group, were associated with fast prevailing streamflow components, small BFI values and short delay times.

To understand if both systems were affected by dry spell temporal variation to the same extent, a simulation approach was used where, given the generation of daily rainfall time series characterized by different average dry spell, the total discharge of the investigated catchments was computed in response to the generated rainfall scenarios, and BFIs were extracted by the application of a hydrograph filtering algorithm.

The primary findings of this study will help to elucidate the extent to which catchment properties can mitigate climate fluctuations and to determine which catchment properties are most meaningful for this purpose.

2. BFI ASSESSMENT FOR OBSERVED CATCHMENTS

2.1 Data description

Because the current investigation is focused on the impact of dry spell characterization on BFI assessment, the observed catchments were principally selected to provide a broad spectrum of climate conditions covered by a north-south European transect from extremely dry and seasonal types (typically in southern Europe) to temperate and oceanic types (typically in northern Europe). Moreover, because this study was concerned with BFI assessment, catchments were also selected to provide a broad range of BFI values and the correspondingly broad range of catchment delay times. According to these rules, daily streamflow, rainfall and temperature data were collated for 10 catchments across Europe from local water agencies or as part of previous studies (Brauer et al., 2011; Van Lanen and Dijksma, 1999; Van Huijgevoort et al., 2011; Mehaiguene et al., 2012; Van Loon and Van Lanen, 2013; Longobardi and Villani, 2013). The locations of the investigated catchments are indicated in Figure 1.

Catchment areas vary between 6.5 and 16500 km^2, and mean catchment elevation ranges between 165 and 1060 m.a.s.l. The range of average annual precipitation is 347–1588 mm, with the largest values occurring for a humid region in southern Italy (Longobardi et al., 2016). Climate regime indications are provided with reference to the Köppen-Geiger climate classification (Figure 1; Peel et al., 2007). A typical mean monthly rainfall distribution is provided in Figure 1 for each of the investigated regions. Climate regimes range from dry type B to temperate type C classes. Semi-arid (Bsk) climates and Mediterranean climate conditions (Csa-Csb) are observed in the southern area of the investigated domain and are characterized by a rather marked seasonal distribution. Temperate oceanic climate conditions (Cfb) prevail in the northern area of the domain and are characterized by a more uniformly distributed precipitation regime. Average annual runoff ranges between 22 and 1309 mm/yr, and none of the catchments shows important snow accumulation and melt processes. Bedrock permeabilities (derived from the Global Hydrogeology MAPs product; Gleeson et al., 2014) range between 10^{-4} and 10^{-9} m/s, ranging from high to extremely low values,. Soil types range from podzols to cambisols to calcisols according to the FAO classification (Soil Atlas of Europe, 2005). More information is provided in Table 1.

2.2 Baseflow separation

Hydrograph components separation was performed to assess the catchment long-term BFI. Following the definition of the Institute of Hydrology (1980), a BFI value was assessed as the ratio between the volume of baseflow and the volume of total streamflow; to derive the baseflow volume, baseflow separation was performed for each catchment.

At least three main categories of separation algorithms can be cited: empirical, digital filter-based and model-based techniques. Each procedure is, to a large extent, arbitrary (Hewelett and Hibbert, 1967) but provides a repeatable methodology to derive objective measures or indices related to a particular streamflow source. Recursive digital filters (RDF) are the most commonly used methods for estimating baseflow because of their simplicity and quick implementation, which only needs streamflow data (Eckhardt 2005; Aksoy et al., 2009; Li et al., 2014), even though RDF parameters are questionable in certain cases, and geochemical or isotopic method calibration would improve the separation between slow and fast components (Lott and Stewart, 2013; Longobardi et al., 2016). Among RDFs, the Lyne and Hollick method (Lyne and Hollick, 1979; Ladson et al., 2013) seemed to be the most flexible approach and to have better performance for a wide range of climate conditions and catchment properties (Li et al., 2014, Longobardi et al, 2016). Because of these reasons, the Lyne and Hollick filter was selected for this study as a simple smoothing and separation rule to separate the baseflow from the total streamflow hydrograph. The Lyne and Hollick method acts as a low-pass filter to remove the high frequency quickflow component of streamflow from the low frequency baseflow component. The filter equation predicts the quickflow q_q component at a time step t by

$$q_q(t) = \alpha q_q(t-1) + \frac{1+\alpha}{2}\left[q(t) - q(t-1)\right], \qquad (1)$$

subject to the restriction $q_q > 0$, where α is the filter parameter that affects the degree of attenuation. The baseflow component q_b at time step t is the difference between total streamflow q and quickflow q_q:

$$q_b(t) = q(t) - q_q(t), \quad (2)$$

subject to the restriction $q_b \leq q$. According to Nathan and McMahon (1990), the value of the filter that yields the most acceptable results in term of baseflow separation is in the range of 0.9 to 0.95. The filter was passed over the data three times, forward, backward and forward again, for a larger smoothing effect, as suggested by Nathan and McMahon (1990).

The result of the assessment is illustrated in Table 1. The BFI showed a large range for the studied catchments, varying from 20% to 80%. The correlation between the BFI and catchment area (8%), mean annual precipitation (3%) and mean annual runoff (3%) appears not relevant. Although not significant, a larger positive correlation (43%) appeared between BFI and the permeability values reported in Table 1. Geo-hydrological soil properties are tightly related to the BFI, and the weak numerical correlation extent found in the current analysis was probably because the permeability values indicated in Table 1 did not account for soil properties and were primarily derived from bedrock type.

3. CHARACTERISTIC SCALE IDENTIFICATION

As discussed in the introduction, BFI vulnerability to dry spell length variation was investigated as a function of two characteristic time scales: the catchment delay time “Ks” and the dry spell length “d”. The first scale parameter helps to distinguish between catchments based on catchment characteristics, particularly between poorly and well-drained catchments. The second scale parameter helps to distinguish between catchments on the basis of climate characteristics. The mentioned scales were identified by a modelling approach which was subsequently used to investigate the mutual interaction between climate and catchment properties.

3.1 Daily streamflow modelling

In view of the modelling analysis that will follow, it is particularly interesting and also conceptually important to differentiate the catchments based on their hydrological response times. A high number and broad range of rainfall-runoff models are available for this aim. Popular physically based models were not considered in this study; simple conceptual approaches have instead been preferred, because although minimal in terms of model input and parametrization, they are able to capture catchment behaviour for highly different climate and basin properties. Among the conceptual rainfall-runoff models, the IAHCRES transfer function approach was selected (Jakeman and Hornberger, 1993). According to a large number of scientific papers, IHACRES appears to be a flexible and versatile model that has been applied to a very broad range of purposes from traditional streamflow prediction (Razavi and Coulibaly, 2013), water resources management (Alredaisy, 2011), and water quality studies (Letcher et al., 2002) to reservoir operating rules management (Ahmadi et al., 2014). Studies exploring the role of climate changes and land cover changes on the hydrological response have also applied IHACRES (Evans and Schreider, 2002; Croke et al., 2004, Aronica and Bonaccorso, 2013).

The IHACRES model accounts for the non-linearity in the catchment response by a rainfall loss filter module driven by climatic forcing. Further down, a routing module considers the existence of two streamflow pathways, slow and fast, that contribute with different weights (time of delay and relative volumetric throughput) to total streamflow based on catchment characteristics. The conceptual separation between slow and fast paths enables the user to characterize the delay times for both streamflow components. The slow path delay time Ks was used in the current study to quantify the hydrological response characteristic time scale.

To test the ability of the model to describe the catchment hydrological behaviour under the climate and geology gradient considered in this study, the model was applied to the 10 catchments under investigation and its performance was measured in terms of the following statistics. Slow flow component delay time (Ks) and slow flow component volumetric throughput coefficient (vs) are illustrated in Table 2. Statistics used to measure model performance were the NSE (Nash and Sutcliff Efficiency coefficient), the coefficient of determination (r^2), the LNSE (Nash and Sutcliffe Efficiency with logarithmic values), and d (index of agreement; Willmott et al., 1985). Because the catchment vulnerability to dry spell length variability was quantified in terms of long-term BFI changes, it was important to understand how reasonable the BFI values provided by the modelling approach were. To quantify such a feature, BFI_{cal}, the BFI value obtained by filtering the modelled time series after calibration, and the BFI relative error percentage between the BFI (computed for observed time series) and BFI_{cal} were also estimated. Metrics estimation is provided in Table 2.

Overall model performance appeared rather satisfactory. Average NSE was approximately 0.7 (min 0.67), average r^2 was approximately 0.85 (min 0.81), average LNSE was approximately 0.66 (min 0.45) and average D was approximately 0.73 (min 0.63). The relative percentage error between the BFI computed for the observed time series and the BFI_{cal} computed for the modelled time series was negligible with an average value of approximately 6%. There was no systematic bias in the BFI model results with both positive and negative deviations from observed values (Table 2) The need to use a specific simulation approach that provided optimal results for the different climate and catchment property conditions was considered and thus appears to be congruent with the selected model.

3.2 Daily rainfall modelling

The characteristic time scale for climate settings is the dry spell d, the period between two consecutive rainfall occurrences. A stochastic point process approach was adopted to describe and assess the characteristic time scale for each of the investigated catchments and for the subsequent generation of daily rainfall series to be used as inputs in the following simulation analysis. The daily rainfall time series were modelled as stochastic Poisson processes with rectangular pulses (PRP) (Rodriguez-Iturbe et al., 1987). The arrival times of daily rainfall storms were assumed to follow a Poisson process of rate λ such that the dry spells were independently and identically distributed as exponential random variables with mean d=1/λ days. Rainfall intensity at time t was obtained as the sum of intensities of all overlapping storms that occurred at that time, which could be generated for each storm occurrence marked by the Poisson process. Rainfall intensity had an exponential distribution with parameter μ.

Average d duration for the studied catchments ranged between a minimum of approximately 3 days (HUP - Cfb) and a maximum of approximately 14 days (PLA - Csa) from northern to southern latitudes (Table 3). Rainfall intensity ranged between approximately 1 mm/d (DJE - Bsk) and 4.36 mm/d (BUS – Csa, Csb), with a relatively lower dependence on a catchment's geographical coordinates (Table 4).

For the successive simulation analyses it was important to confirm the suitability of the PRP approach for the case studies. To assess the goodness-of-fit for the studied data, main descriptive statistics (mean, maximum, standard deviation) for observed and modelled daily rainfall were quantified and are reported in Table 3 and Table 4. Additionally, observed and modelled daily rainfall cumulative distributions were compared with the use of the average absolute percentage error (AAPE), defined as

$$AAPE = \frac{1}{n}\sum_{i=1}^{n}\left|\frac{F_{obs,i} - F_{\mathrm{mod},i}}{F_{obs,i}}\right| \qquad (3)$$

where i is the percentile order, $F_{obs,i}$ is the cumulative distribution for observed daily rainfall corresponding to the i-th percentile, $F_{mod,i}$ is the cumulative distribution for modelled daily rainfall corresponding to the i-th percentile, and n is the number of percentiles. AAPE values are also reported in Table 3 and Table 4.

Overall model performance appears to have been rather satisfactory. The d process, which is of particular interest in the current research, appears to have been well represented. Errors in cumulative distribution fitting were smaller than 10% for half of the catchments and not larger than 25% for the remaining catchments (Table 3). Beyond mean values, the maximum values for dry spell lengt also appeared congruent with the observations (Table 3). Similar comments hold for the rainfall intensity, with a moderate increase in the goodness-of-fit errors (Table 4).

4. THE RELATION BETWEEN OBSERVED CATCHMENT BFI, CATCHMENT DELAY AND DRY SPELL

For the number of investigated catchments, Ks ranged between approximately 30 days (HUP) to 200 days (NOO), as reported in Table 2. When BFI values were plotted against Ks values, catchments appeared to have been naturally forced into two clusters as indicated in Figure 2, where the empirical relation between Ks and BFI is illustrated.

The well-drained group was characterized by a delay time longer than 80 days and BFI values larger than 0.5. Within this group, the empirical relationship Ks-BFI showed increasing BFI for increasing delay times. Larger Ks (larger BFI) values generally occurred for high permeability and/or high water holding capacity soils (Table 1). The poorly-drained group was characterized by delay times shorter than 80 days and BFI values smaller than 0.5. For this group, the empirical relationship Ks-BFI was not as evident as in the well-drained one because catchments having similar response delay times were associated with very different BFI values. For example, the Platis (PLA) and Hupsel (HUP) catchment delay times were approximately 44 days and 30 days, respectively, but the BFI for HUP was 50% larger than the BFI for PLA. Lower Ks (lower BFI) values were generally associated with low permeability and low water holding capacity soils (Table 1).

The empirical relationship between d and the BFI was less clear because the same values of d related to extremely different BFI values (Figure 3). Groups were indeed still noticeable, but they were primarily driven by the BFI value, and poorly-drained catchments lay respectively above and below the threshold of BFI = 0.5. Within each group, although it was more evident for the well-drained group, a more uniform precipitation distribution represented by a small value of d, typical in medium to northern latitude climates, related to larger BFI. As an example, the Platis (PLA) and

Hupsel (HUP) difference in BFI assessment previously cited seems to be justified by their relative d values; the Hupsel catchment was indeed forced by more uniform precipitation occurrences, which made the related hydrological regime more persistent and subsequently yielded a larger BFI value compared with the Platis catchment.

The coevolution of climate and geology is not new to the scientific literature (Troch et al., 2015). Both at plot and regional scales, climate features control soil development and soil properties (Lavee et al., 1997) to the point that climate changes are supposed to affect and induce changes in hydro-geomorphological processes (Lane, 2013). Catchment delay times are frequently considered as constant parameters and related to catchment properties; however, for a more realistic simulation, particularly of the baseflow time series, concern has been raised about a dependence on the climate regime properties (He et al., 2016; Longobardi et al., 2016). The dataset used for the current analysis empirically depicts such a relation, although it represents a small sample (Figure 4). Although rather scattered, a tendency seems to appear in Figure 4 where the larger the d, the smaller the Ks (the less uniform the precipitation regime, the less persistent the hydrological regime). The Hupsel catchment represents an exception to the rule, probably because of the combination of very low permeability and small drainage area.

Soil and geological properties and climate effects on the baseflow properties could be individually considered only to a limited extent because they have the potential to impact each other and mitigate the relevant effects. To summarize their mutual impact on the BFI, the ratio between the characteristic time scales could be considered, that is, d/Ks.

If the BFI is in fact plotted against the d/Ks values, the existence of well- and poorly-drained groups resulted in an almost univocal relation, such as for the case of Ks dependence (Figure 2); however, in this case, the impact of d was also considered (Figure 5). In fact, this pattern enabled the group definitions to be maintained and the BFI values to be sorted as an inverse decreasing function of d/Ks. Large d/Ks values defined the domain of catchments where d and Ks were of the same order of magnitude. Poorly-drained catchments were located in this section with BFI values of approximately 25%. Inversely, low d/Ks values defined the domain of catchments where d << Ks. Well-drained catchments were located in this section, with a BFI larger than 60% being observed.

The use of the ratio d/Ks in the description of the BFI variability also quantitatively strengthens the dependence of this index on the characteristic time scales identified. By using a regression model to explain the variability of the BFI with respect to the Ks parameter alone, we find that the variance explained is very high in the case of the well-drained group (85%) and very low in the case of the poorly-drained group (22%). Using instead the ratio d/Ks, the variance explained with respect to the whole set of basins is equal to 85%.

If the introduction of the weight d on Ks does not appear significant for the well-drained group, it made it possible to distinguish between poorly-drained catchments with the same hydrological properties but different climate parameters.

The representation provided in Figure 5 justifies indeed the previously mentioned observed differences between HUP and PLA, assigns them significantly different d/Ks ratios, and embeds the significant differences in terms of d.

5. MODELLED IMPACT OF DRY SPELL DURATION ON OBSERVED CATCHMENT BFIs

Next we used a simulation approach to measure how changes in dry spell length propagate through the catchment response to produce changes in the BFI values. Changes in d included both a decrease (wetter conditions) and an increase (drier conditions) in d. Each of the catchments in Table 1 is characterized by a deterministic catchment response; the hydrological model parameters (Table 2) were thus kept constant, as well as the slow path delay time Ks. For each of the catchments, several daily rainfall scenarios were generated according to the PRP model, each characterized by a different value for d. The parameter range for d was based on the empirical study, which covered an exhaustive gradient of climate conditions. The average daily d was assumed to vary between 3 and

16 days To compare catchments, only increases or decreases of 20% and 50% of the initial d value were considered in the modelling exercise (Figure 6).

Generated rainfall scenarios were then used to force the IHACRES model to simulate the catchment response, and the Lyne and Hollick algorithm was used to derive the baseflow series from the simulated total streamflow series to quantify the BFI index. Overall, an increase in d, that is a shift towards drier conditions, led to a decrease in the BFI (Δdry); in contrast, a decrease in d, that is a shift towards wetter conditions, led to an increase in the BFI (Δwet). Catchment vulnerability was measured by

$$maximum\ percentage\ BFI\ increase = \frac{\Delta wet}{BFI_{\bar{d}}} = \frac{BFI_{d^{-\%}} - BFI_{\bar{d}}}{BFI_{\bar{d}}}\ (\%) \qquad (4)$$

and

$$maximum\ percentage\ BFI\ decrease = \frac{\Delta dry}{BFI_{\bar{d}}} = \frac{BFI_{\bar{d}} - BFI_{d^{+\%}}}{BFI_{\bar{d}}}\ (\%) \qquad (5)$$

where $\bar{d}$ represents the initial d value, $d^{-\%}$ represent the 20% (or 50%) reduced value for $\bar{d}$ and $d^{+\%}$ represents the 20% (or 50%) increased value for $\bar{d}$. In the following, we only considered as significant a variation in BFI larger than 10%.

The behaviour of poorly-drained and well-drained groups was different, and the main findings are summarized below.

A 20% decrease in $\bar{d}$ values did not produce changes in BFI for any of the studied catchments, a 50% decrease generated BFI increases up to 20% (Figure 7 – left panel). Poorly-drained catchments appear the most vulnerable as they are associated with the largest maximum percentage BFI increases. Within this group, catchments with a combination of small Ks and large $\bar{d}$ (large d/Ks values) appear to be the most affected (Figure 7 c)). Catchments located at the opposite boundary, low d/Ks (large Ks and small $\bar{d}$), were almost unresponsive to a decrease in dry spell length. The same could be said in the case of a shift toward wetter condition, where 20% and 50% $\bar{d}$ increases generated almost similar effects on the studied catchments (Figure 7 – d), e) and f)).

The unexpected behaviour of some catchments in this analysis can be explained by soil properties. This is for example the case of the Sele watershed, SEL, which is among the class of well-drained the only catchment to be significant affected by variation in d (Figure 7 c)). Although in the group classification based on Ks SEL clearly belongs to the well-drained group (Figure 2), if the d/Ks ratio is used, SEL lays in the d/Ks range typical for the poorly-drained group (Figure 5). Different from the other well-drained catchments, SEL bedrock permeability was not very large, and the large BFI value (0.54), which forces SEL into the well-drained group, was probably generated by the presence of very important alluvial deposits, rather than by large bedrock permeability. Soil properties can also explain the difference between the Djidiouia (DJE) and Platis (PLA) watersheds (Figure 7 f)). Characterized by similar values for Ks and d (and consequently d/Ks) and by the same bedrock permeability (Table 1), PLA and DJE differed in terms of soil types, which were leptosols and calcisols, respectively. The capacity of leptosols to hold water and contribute to baseflow generation is low, which may have led to the BFI decrease detected by the simulation

6. INFLUENCE OF DRY SPELL DURATION ON BFI IN SIMULATED VIRTUAL CATCHMENTS

To support and further expand the results provided by the analysis of the observed catchments, the hydrological behaviour of a very broad set of virtual catchments was investigated.

The observed catchments selected for the current study covered a broad spectrum of climate conditions, ranging from extremely dry and seasonal climate types to temperate and oceanic climate types. The catchments also covered a broad range of BFI values and corresponding catchment delay times (tightly related to BFI as shown in Figure 2). Assuming that the selected catchments cover the range of hydrological catchment behaviours existing in Europe, the maximum and the minimum values of the PRP and IHACRES model parameters calibrated for the observed catchments were used as the range of model parameters (both PRP + IHACRES) in the synthetic simulation. These simulations were used to generate synthetic streamflow time series for above two thousand “virtual catchments” (Table 5). The virtual catchment behaviour was studied in terms of BFI assessment and its variability with the d/Ks parameter.

Although a good correspondence was found between observed and virtual catchments, the BFI-d/Ks domain described by the virtual catchments (Figure 8) extended beyond the range of the observed catchments, which strengthened the significance of the findings, especially concerning the d/Ks parameter.

According to Figure 8 (upper right panel), for a given d value, the effects of Ks on the BFI was practically negligible for the poorly-drained group; a long and narrow tail in the BFI-d/Ks domain was recognized for large d/Ks values, which corresponded to the lower range for Ks. The effect became more important for the well-drained group because the spread of the BFI-d/Ks domain significantly increased from larger to smaller d/Ks.

For a given value of Ks (Figure 8 right lower panel) the effect of d on the BFI assessment, measured by the width of the domain, appeared important for the well-drained group (lower d/Ks values) and particularly for values included in the interval 0.1-0.3, where the extent of the domain appeared wider. The importance of d on BFI assessment was drastically reduced for the poorly-drained group (large d/Ks values, larger than 0.6), for which BFI values were within the minimal range of 0.1-0.2 regardless of the d values.

Similarly to what represented for the observed catchments in Figure 7, Figure 9 illustrates the maximum percentage BFI increase or decrease for the dataset of virtual catchments due to a decrease and an increase in the dry spell length. The results found for the virtual catchments appear congruent with the finding from observed catchments. A 50% decrease in d produces larger effect than a 20% decrease, whereas the effect of a 20% and a 50% increase are similar in terms of BFI changes. Larger changes are also in this case detected for large d/Ks.

It has to be noted however that the use of a percentage decrease or increase of the initial value of d, e.g., 20% and 50%, considered in the current analysis, implies that systems characterized by small initial d values see a smaller absolute change in d (and d/Ks) than systems characterized by a large value of initial d. As an example, Figure 10 shows the modelled BFI variability for a set of virtual catchments featured by two extremely different initial d values and subject to the same 50% d decrease. Systems featured by the same Ks values exhibit a significantly different behaviour depending on their initial state. In the case of the lower Ks (the poorly-drained group) starting from a dry initial condition (large d) leads to a 30% overestimation of BFI variability compared to the case of wet initial conditions (red boxes in Figure 10). Differences are evidently dampened in the case of large Ks (the well-drained group, blue triangles in Figure 10). The range of variability of the d/Ks parameter is furthermore significantly larger in the case of initial dry conditions.

As this effect might distort the assessment of the impact of d variability on the BFI, the maximum BFI increase and decrease were standardized by a measure of variability of the d/Ks index, the standard deviation of the d/Ks (Figure 11). The simulation experiments showed that, even though under the same dry spell variation, the BFI vulnerability appeared higher for catchments poorly-drained systems, attributing an equal weight to the variations in d both in the case of dry and wet initial conditions, for tendencies towards both wetter and drier climates, the poorly-drained systems appear to have been less impacted by climate fluctuation than the well-drained systems.

To further support the results, the BFI vulnerability can be additionally studied in terms of BFI variability, the BFI standard deviation, beyond the maximum percentage increase/decrease. Figure 12 indicates even more clearly how the impact on BFI variability decreases for large d/Ks ratios, thus for the poorly-drained group. In particular the maximum variability in standardised BFI was approached for a d/Ks values that correspond to the limit of transition between the well-drained and the poorly-drained groups as illustrated for the observed catchments in Figure 5.

7. CONCLUSIONS

In a combined data-based and modelling study, where the hydrological behaviour of observed and virtual catchments was investigated over a broad gradient of climate conditions and catchment properties, we aimed to illustrate the impact of climate variability and, in particular, the impact of dry spell duration on the baseflow process, as summarized by the BFI index.

An index based on the combination of catchment and rainfall properties, d/Ks, the ratio between the dry spell length and the catchment delay time, was used to group catchments into well- and poorly-drained groups and to measure the variability of the BFI index for a given rate of dry spell variability.

As a general rule, the effect of the main hydrological parameter Ks on the BFI was practically negligible for the poorly-drained group and became more important for the well-drained group as the spread of the BFI-d/Ks domain significantly increased from larger to smaller d/Ks. The impact of d on the BFI, as measured by the width of the domain BFI-d/Ks, appears to be important for the well-drained group (lower d/Ks values) and drastically reduced for the poorly-drained group (large d/Ks values, larger than 0.6), for which BFI values were set to minimal values regardless of the d values.

With respect to the climate fluctuation and in particular an increase or decrease in dry spell length, the tendency towards drier climates (extension of dry spell length) appears to have caused minor hydrological impact, compared with the tendency towards wetter climates. The simulation experiments further showed how, for tendencies towards both wetter and drier climates, the poorly-drained systems appear to have been less impacted by climate fluctuation than the well-drained systems and that the impact reached maximum values for systems laying in the transition zone between well- and poorly-drained systems.

Although the virtual catchment behaviour enabled the assessment of general patterns of BFI vulnerability, the study of the observed catchments provided a thorough knowledge of the hydrological systems and shed light on the role of specific hydrological parameters, that is, the catchment properties, on BFI assessment.

It is important to stress that the reported effects on the BFI variability produced by the variability in the dry spell length do not represent the impact of climate variations on the full spectrum of the low flow hydrological regime but on only one of the indices to be used to classify the low flow regime. Being a long-term average index, the BFI is probably moderately sensitive to changes towards more-or-less extreme climate conditions, but it is not insensitive, and future research on indices that describe more extreme low flow features could show even more marked results.

Acknowledgements:

The authors would like to thank the associate editor and the anonymous reviewers for their valuable comments and suggestions that resulted in an improvement of the current research work.

The authors would also like to thank the people who contributed to data provision, in particular, Claudia Brauer (Wageningen University) for Hupsel data, Roel Dijksma (Wageningen University) for Noor data, the Guadiana Water Authority, CEDEX, and AEMET for Guadiana data, Aristeidis Koutroulis (Technical University of Crete) for Platis data and Madjid Mehaiguene (Khemis Milian University) for Djidiouia data. The authors also thank Henny Van Lanen (Wageningen University) and Marjolein Van Huijgevoort (KWR Water) for their encouraging discussions in planning the research experiments. Funding from NWO grant 2004/08338/ALW and the Research Italian Ministry (MIUR) under the grant ORSA154528 and ORSA164189 are gratefully acknowledged.

REFERENCES

Ahmadi, M., Haddad, O.B., Loáiciga, H.A. (2014). Adaptive Reservoir Operation Rules Under Climatic Change. Water Resources Management, 29 (4), 1247-1266.

Aksoy, H., Kurt, I., Eris, E. (2009) .Filtered smoothed minima baseflow separation method. Journal of Hydrology, 372 (1-4), 94-101.

Alredaisy, S.M.A. (2011). Recommending the IHACRES model for water resources assessment and resolving water conflicts in Africa. Journal of Arid Land, 3 (1), 40-48.

Aronica, G.T., Bonaccorso, B. (2013). Climate change effects on hydropower potential in the Alcantara River basin in Sicily (Italy). Earth Interactions, 17 (19).

Arnell, N.W., Gosling, S.N. (2013). The impacts of climate change on river flow regimes at the global scale. Journal of Hydrology, 486, 351-364.

Beck, H. E., van Dijk, A. I. J. M., Miralles, D. G., de Jeu, R. A. M., Bruijnzeel, L. A., McVicar, T. R., and Schellekens, J. (2013). Global patterns in baseflow index and recession based on streamflow observations from 3394 catchments. Water Resources Research, 49, 7843–7863.

Bejarano, M.D., Marchamalo, M., Garcia de Jalon, D., Gonzalez del Tanago, M. (2010). Flow regime patterns and their controlling factors in the Ebro basin (Spain). Journal of Hydrology 385, 323-335.

Berhanu, B., Seleshi, Y., Demisse, S.S., Melesse, A.M. (2015). Flow regime classification and hydrological characterization: A case study of Ethiopian rivers. Water (Switzerland), 7 (6), 3149-3165.

Botter, G., Basso, S., Rodriguez-Iturbe, I., Rinaldo, A. (2013). Resilience of river flow regimes. Proceedings of the National Academy of Sciences of the United States of America, 110 (32), 12925-12930.
Coopersmith, E.J., Minsker, B.S., Sivapalan, M. (2014). Patterns of regional hydroclimatic shifts: An analysis of changing hydrologic regimes. Water Resources Research, 50 (3), 1960-1983.
Croke, B.F.W., Merritt, W.S., Jakeman, A.J. (2004). A dynamic model for predicting hydrologic response to land cover changes in gauged and ungauged catchments. Journal of Hydrology, 291 (1-2), 115-131.
Crooks, S.M., Kay, A.L. (2015). Simulation of river flow in the Thames over 120 years: Evidence of change in rainfall-runoff response? Journal of Hydrology: Regional Studies, 4 (PB), 172-195.
Doulatyari, B., Betterle, A., Basso, S., Biswal, B., Schirmer, M., Botter, G. (2015). Predicting streamflow distributions and flow duration curves from landscape and climate. Advances in Water Resources, 83, 285-298.
Eckhardt, K. (22005). How to construct recursive digital filters for baseflow separation. Hydrological Processes, 19 (2), 507-515.
Evans, J., Schreider, S. (2002). Hydrological impacts of climate change on inflows to Perth, Australia. Climatic Change, 55 (3), 361-393.
Gleeson, T., N. Moosdorf, J. Hartmann,and L. P. H. van Beek (2014). A glimpse beneath earth's surface: Global HYdrogeology MaPS (GLHYMPS) of permeability and porosity. Geophysical Research Letters, 41, 3891–3898.
Gustard, A., Roald, L., Demuth, S., Lumadjeng, H. and Gross, R. (1989). Flow regimes from experimental and network data (FREND). 2 Vols. Institute of Hydrology, Wallingford, U.K.
He, S., Li, S., Xie, R., Lu, J. (2016). Baseflow separation based on a meteorology-corrected nonlinear reservoir algorithm in a typical rainy agricultural watershed. Journal of Hydrology, 535, 418-428.
Hewelett, J.D., Hibbert, A.R. (1967). Factors affecting the response of small watershed to precipitation in humid areas. In International Symposium of Forest hydrology, Pergammon press, 275-290.
Institute of Hydrology, 1980. Low Flow Studies (1–4), Wallingford, UK.
Jakeman, A.J. and Hornberger, G.M. (1993). How much complexity is warranted in a rainfall-runoff model? Water Resources Research, 29, 2637–2649.
Jacob, D., Petersen, J., Eggert, B., Alias, A., Christensen, O.B., Bouwer, L.M., Braun, A., Colette, A., Déqué, M., Georgievski, G., Georgopoulou, E., Gobiet, A., Menut, L., Nikulin, G., Haensler, A., Hempelmann, N., Jones, C., Keuler, K., Kovats, S., Kröner, N., Kotlarski, S., Kriegsmann, A., Martin, E., van Meijgaard, E., Moseley, C., Pfeifer, S., Preuschmann, S., Radermacher, C., Radtke, K., Rechid, D., Rounsevell, M., Samuelsson, P., Somot, S., Soussana, J.-F., Teichmann, C., Valentini, R., Vautard, R., Weber, B., Yiou, P. (2014). EURO-CORDEX: New high-resolution climate change projections for European impact research. Regional Environmental Change, 14 (2), 563-578.
Kennard, M.J., Mackay, S.J., Pusey, B.J., Olden, J.D, Marsh N. (2010). Quantifying uncertainty in estimation of hydrologic metrics for ecohydrological studies. River Research and Applications, 26: 137-156.
Ladson, A.R., Brown, R., Neal, B., Nathan, R. (2013). A standard approach to baseflow separation using the Lyne and Hollick filter. Australian Journal of Water Resources, 17 (1), 25-34.
Lane, S.N. (2013) 21st century climate change: Where has all the geomorphology gone? Earth Surface Processes and Landforms, 38 (1), 106-110.
Lavee H., Imeson, A.C., Sarah, P. (1998). The impact of climate change on geomorphology and desertification along a Mediterranean transect. Land degradation and development, 9, 407-422.
Letcher, R.A., Jakeman, A.J., Calfas, M., Linforth, S., Baginska, B., Lawrence, I. (2002). A comparison of catchment water quality models and direct estimation techniques. Environmental Modelling and Software, 17 (1), 77-85.
Li, L., Maier, H.R., Lambert, M.F., Simmons, C.T., Partington, D. (2013). Framework for assessing and improving the performance of recursive digital filters for baseflow estimation with application to the Lyne and Hollick filter. Environmental Modelling and Software, 41, pp. 163-175.
Li, L., Maier, H.R., Partington, D., Lambert, M.F., Simmons, C.T. (2014). Performance assessment and improvement of recursive digital baseflow filters for catchments with different physical characteristics and hydrological inputs. Environmental Modelling and Software, 54, pp. 39-52.
Longobardi, A., Villani, P. (2013). A statistical parsimonious empirical framework for regional flow duration curve shape prediction in a large permeability Mediterranean region. Journal of Hydrology, 507, 174-185.
Longobardi, A., Buttafuoco, G., Caloiero, T., Coscarelli, R. (2016). Spatial and temporal distribution of precipitation in a Mediterranean area (southern Italy). Environmental Earth Sciences, 75 (3), 189, pp. 1-20
Longobardi, A., Villani, P., Guida, D., Cuomo, A. (2016). Hydro-geo-chemical streamflow analysis as a support for digital hydrograph filtering in a small, rainfall dominated, sandstone watershed. Journal of Hydrology, 539, 177-187.
Lott, D.A., Stewart, M.T. (2013). A Power Function Method for Estimating Base Flow. GroundWater, 51 (3), 442-451.
Lyne, V.D., Hollick, M. (1979). Stochastic time-variable rainfall runoff modelling. In Hydrology and Water Resources Symposium. Institution of Engineers Australia, Perth, pp. 89-92.
Mehaiguene, M., Meddi, M., Longobardi, A., Toumi, S. (2012). Low flows quantification and regionalization in North West Algeria. JJournal of Arid Environments, 87, 67-76.
Muller, M. F., Dralle, D. N., Thompson, S.E. (2014). Analytical model for flow duration curves in seasonally dry climates, Water Resources Research, 50, 5510–5531.
Nathan, R.J., McMahon, T.A. (1990). Evaluation of automated techniques for baseflow and recession analyses. Water Resources Research, 26 (7), 1465-1473.

Olden, J.D., Kennard, M.J., Pusey, B.J. (2012). A framework for hydrologic classification with a review of methodologies and applications in ecohydrology. Ecohydrology, 5 (4), 503-518.

Pascale, S., Lucarini, V., Feng, X., Porporato, A., Hasson, S. (2016). Projected changes of rainfall seasonality and dry spells in a high greenhouse gas emissions scenario. Climate Dynamics, 46 (3-4), 1331-1350.

Peel, M.C., Finlayson, B.L., McMahon, T.A. (2007). Updated world map of the Köppen-Geiger climate classification. Hydrology and Earth System Sciences, 11 (5), 1633-1644.

Rajah, K., T. O'Leary, A. Turner, G. Petrakis, M. Leonard, Westra, S. (2014). Changes to the temporal distribution of daily precipitation, Geophysical Research Letters, 41, 8887–8894.

Razavi, T., Coulibaly, P. (2013). Streamflow prediction in ungauged basins: Review of regionalization methods. Journal of Hydrologic Engineering, 18 (8), 958-975.

Rodriguez-Iturbe, I., Cox, D.R., Isham, V. (1987). Some models for rainfall based on stochastic point process. Proceeding of the Royal Society of London, A 410, 269-288.

Sawicz, K.A., Kelleher, C., Wagener, T., Troch, P., Sivapalan, M., Carrillo, G. (2014). Characterizing hydrologic change through catchment classification. Hydrology and Earth System Sciences, 18 (1), 273-285.

Schneider, M.K., Brunner, F., Hollis, J.M., Stamm, C. (2007). Towards a hydrological classification of European soils: preliminary test of its predictive power for the base flow index using river discharge data. Hydrology and Earth System Science, 11, 1501-1513.

Soil Atlas of Europe, European Soil Bureau Network, European Commission, (2005), 128 pp, Office for Official Publications of the European, Communities, L-2995 Luxembourg

Staudinger, M., Weiler, M., Seibert, J. (2015). Quantifying sensitivity to droughts-an experimental modeling approach. Hydrology and Earth System Sciences, 19 (3), pp. 1371-1384.

Stoelzle, M., K. Stahl, A. Morhard, Weiler, M. (2014). Streamflow sensitivity to drought scenarios in catchments with different geology, Geophysical Research Letters, 41, 6174–6183.

Troch, P.A., Lahmers, T., Meira, A., Mukherjee, R., Pedersen, J.W., Roy, T., Valdés-Pineda, R. (2015). Catchment coevolution: A useful framework for improving predictions of hydrological change? Water Resources Research, 51 (7), 4903-4922.

Van Loon, A.F., Laaha, G. (2015). Hydrological drought severity explained by climate and catchment characteristics. Journal of Hydrology, 526, pp. 3-14.

Willmott, C.J., Ackleson, S.G., Davis, R.E., Feddema, J.J., Klink, K.M., Legates, D.R., ODonnell, J. and Rowe, C.M. (1985). Statistics for the evaluation and comparison of models. Journal of Geophysical Research, 90, 8995–9005.

Zhang, R., Li, Q., Chow, T.L., Li, S., Danielescu, S. (2013). Baseflow separation in a small watershed in New Brunswick Canada, using a recursive digital filter calibrated with the conductivity mass balance method. Hydrological Processes, 27, 2659–2665.

Figure captions

Figure 1: Red frames indicate regions where the investigated catchments are located. Histograms of mean monthly rainfall distribution are illustrated for each region. The Köppen climate classification map is also provided (upper right corner) for identification of climate groups.

Figure 2: BFI dependence on slow storage delay times. Squares define poorly-drained and circles define well-drained catchments.

Figure 3: BFI dependence on average dry spell d. Squares define poorly-drained and circles define well-drained catchments.

Figure 4: Empirical relationship between average dry spell d and slow storage delay time. Squares define poorly-drained and circles define well-drained catchments.

Figure 5: BFI dependence on d/Ks ratio. Squares define poorly-drained and circles define well-drained catchments.

Figure 6: Modelling analysis flow chart.

Figure 7: Maximum percentage BFI decrease or increase as a function of d, Ks and d/Ks. Squares define poorly-drained and circles define well-drained catchments. Light colours define 20% increase or decrease in d; dark colours define 50% increase or decrease in d. Right panel: dry spell length increase. Left panel: dry spell length decrease.

Figure 8: BFI-d/Ks domain for observed (red circles) and virtual catchments (light blue circles). The insets visualizes the effect of model parameters on the spread of the results. Right upper panel: effect of Ks. Right lower panel: effect of d.

Figure 9: Maximum percentage BFI increase (left panels) and decrease (right panels) as a function of d/Ks. Light colours (upper panel) define 20% decrease or increase in d; dark colours (lower panel) define 50% decrease or increase in d.

Figure 10: Modelled BFI variability induced by a decrease in d of 50% in the case of dry initial conditions (large d) and wet initial conditions (small d). Virtual catchments inside red and blue boxes are characterized by the same Ks value.

Figure 11. Ratio between BFI maximum percentage increase and decrease and d/Ks standard deviation for a decrease (left panels) and an increase (right panels) of the dry spell length d. Light colours (upper panel) define 20% decrease or increase in d; dark colours (lower panel) define 50% decrease or increase in d.

Figure 12: Ratio between BFI standard deviation and d/Ks standard deviation for a decrease (left panels) and an increase (right panels) of the dry spell length d. Light colours (upper panel) define 20% decrease or increase in d; dark colours (lower panel) define 50% decrease or increase in d. Plot areas included in the red boxes are enlarged in the adjacent illustrations.

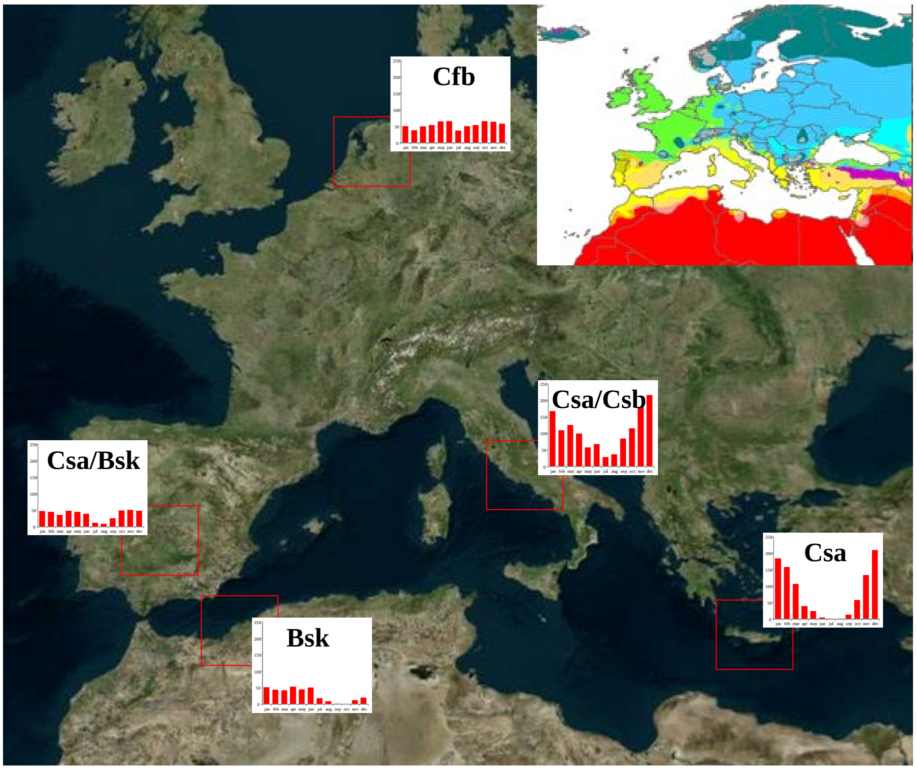

Figure 1. Red frames indicate regions where investigated catchments are located. Histograms of mean monthly rainfall distribution are illustrated for each region. The Köppen climate classification map is also provided (upper right corner) as identification of climate groups.

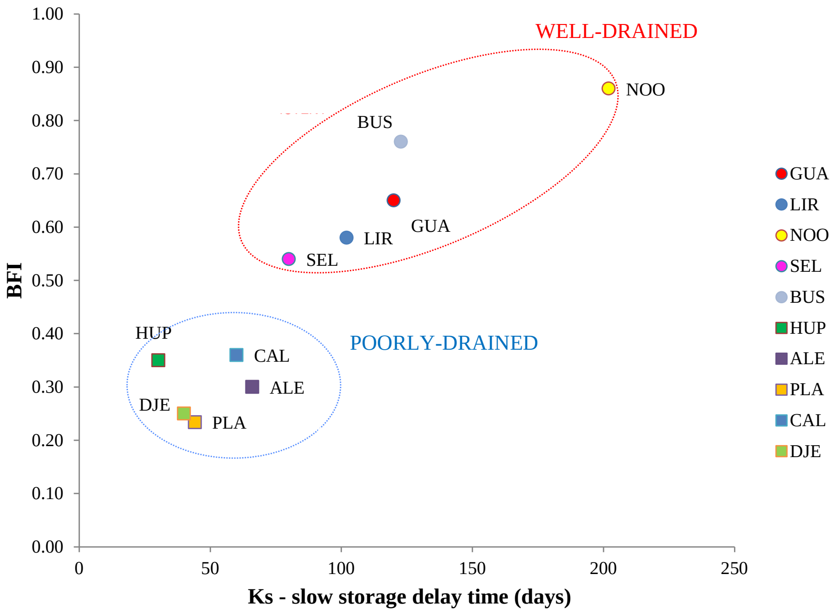

Figure 2. BFI dependence on slow storage delay times. Squares define poorly-drained and circles define well-drained catchments.

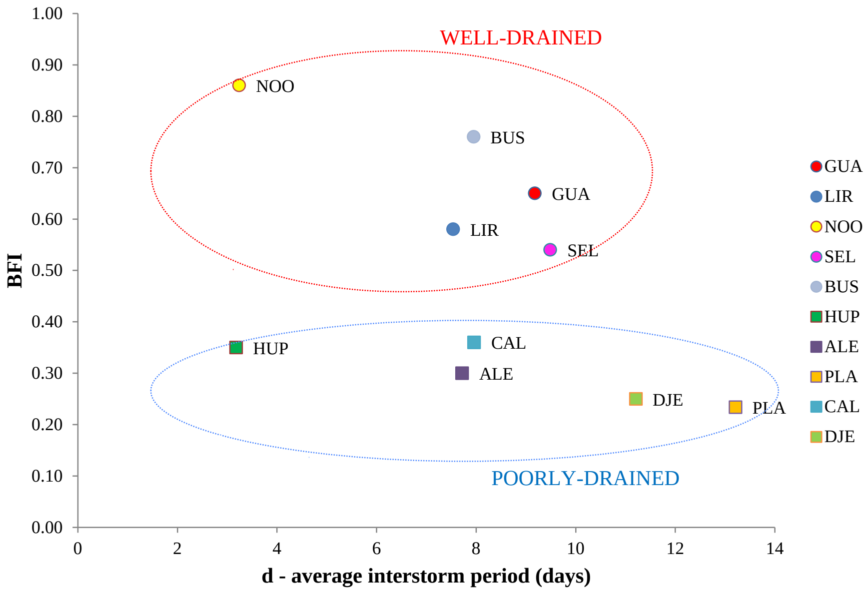

Figure 3. BFI dependence on average dry spell d. Squares define poorly-drained and circles define well-drained catchments.

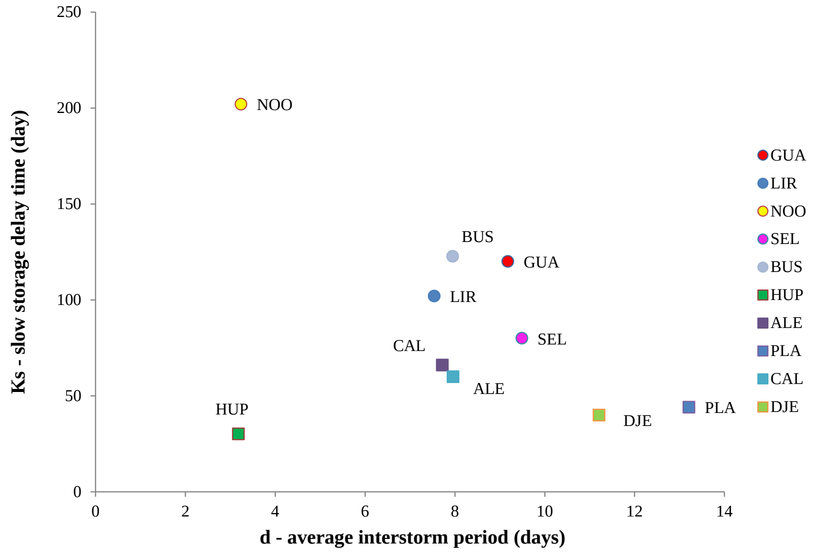

Figure 4. Empirical relationship between average dry spell d and slow storage delay time. Squares define poorly-drained and circles define well-drained catchments.

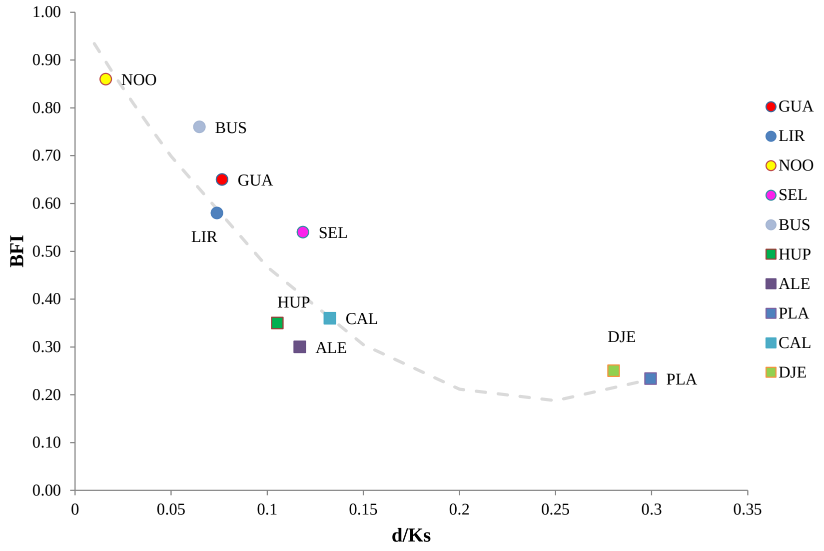

Figure 5. BFI dependence on d/Ks ratio. Squares define poorly-drained and circles define well-drained catchments.

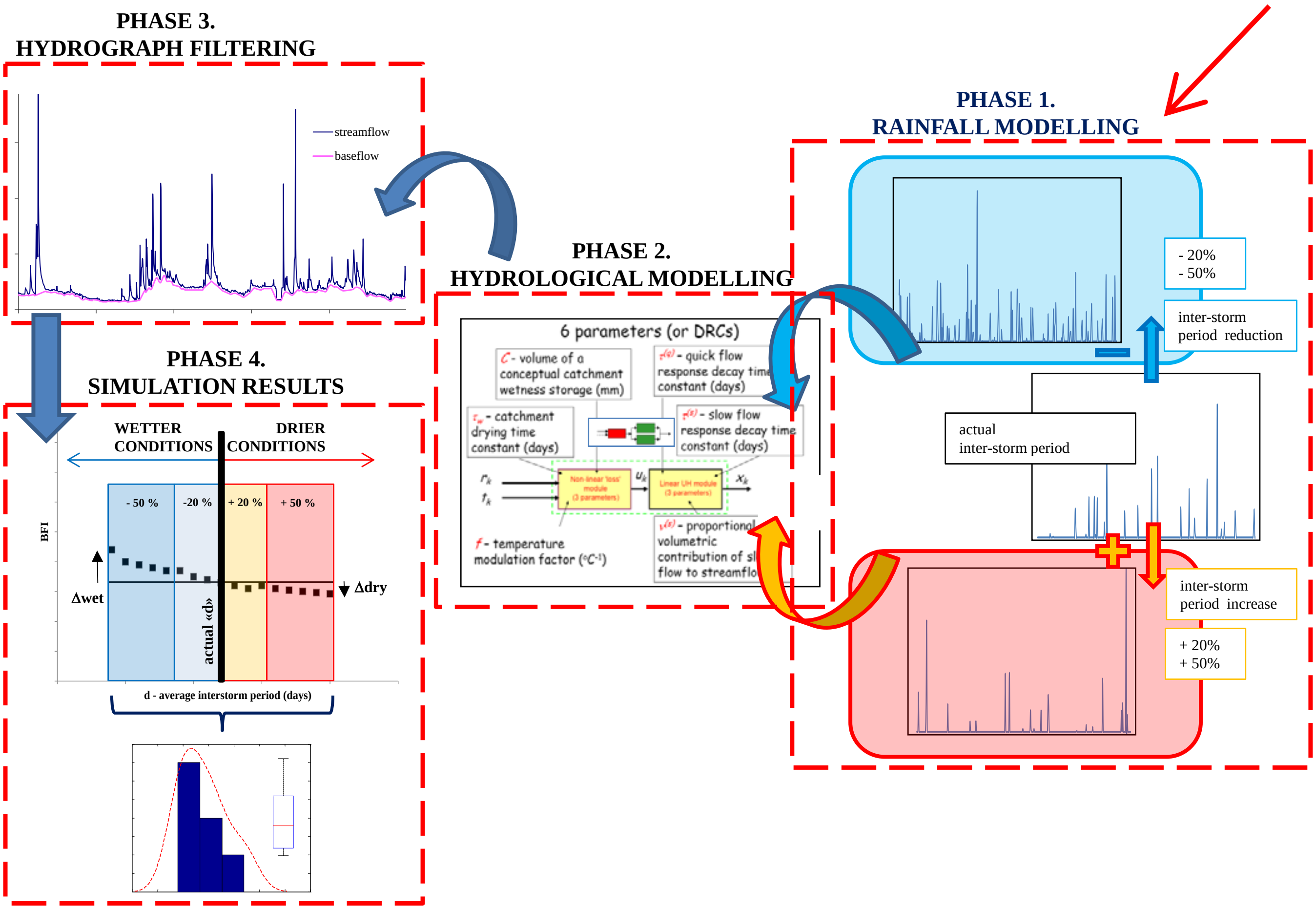

Figure 6. Modelling analysis flow chart.

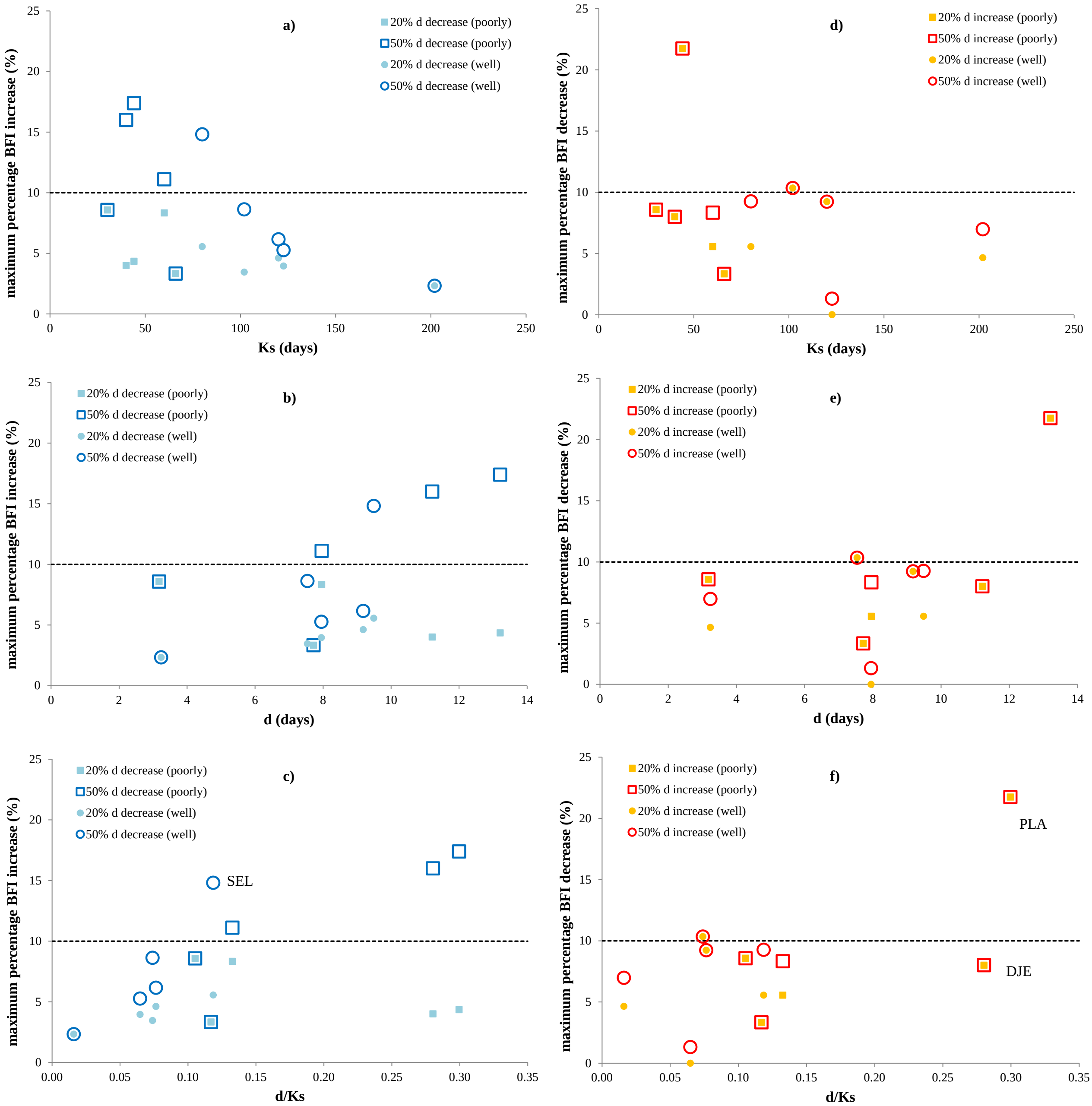

Figure 7. Maximum percentage BFI increase and decrease as a function of d, Ks and d/Ks. Squares define poorly-drained and circles define well-drained catchments. Light colors define 20% increase or decrease in d, dark colors define 50% increase or decrease in d. Right panel: dry spell length increase. Left panel: dry spell length decrease.

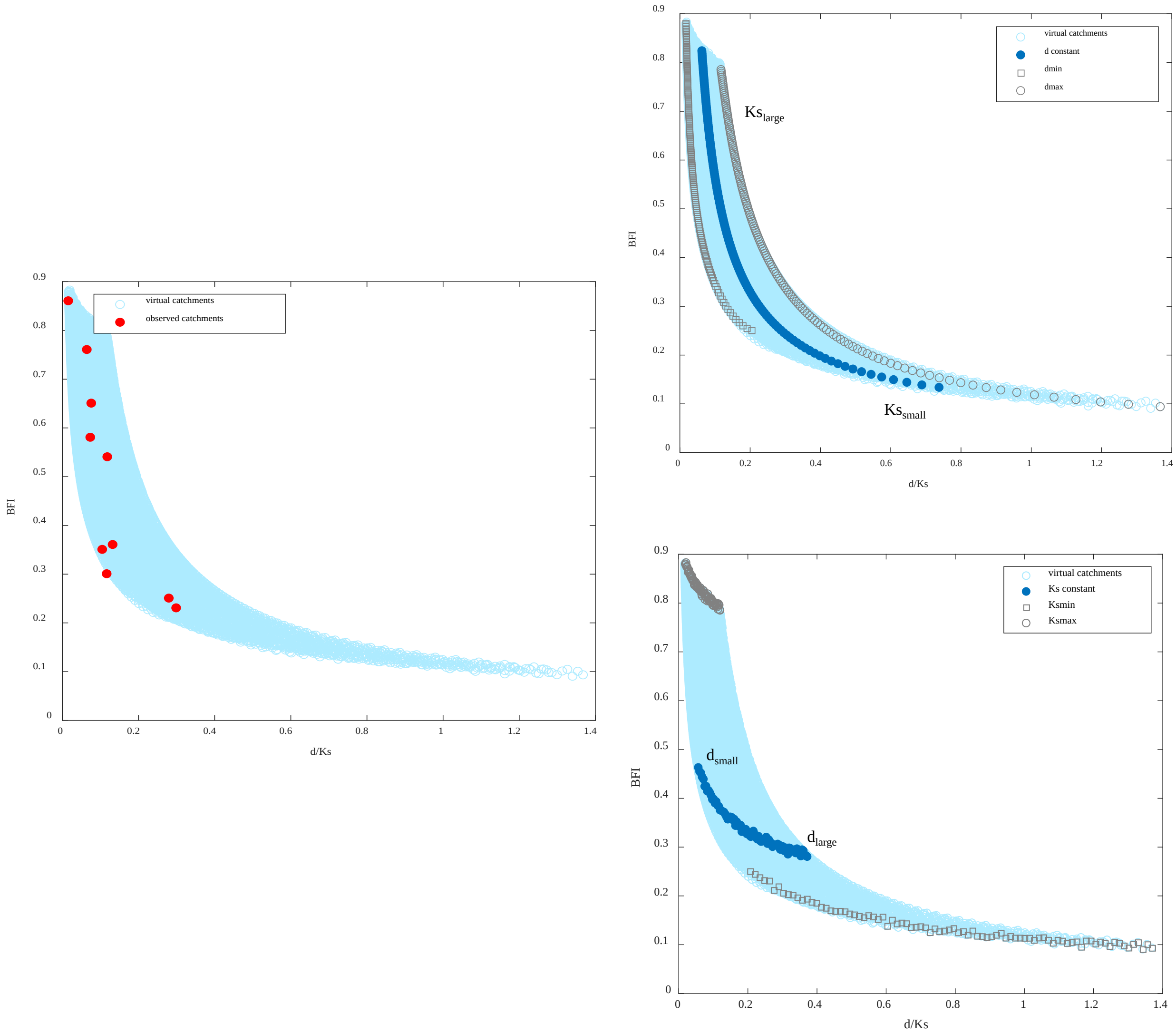

Figure 8. BFI-d/Ks domain for observed (red circles) and virtual catchments (light blue circles). The insets visualizes the effect of model parameters on the spread of the results. Right upper panel: effect of Ks. Right lower panel: effect of d.

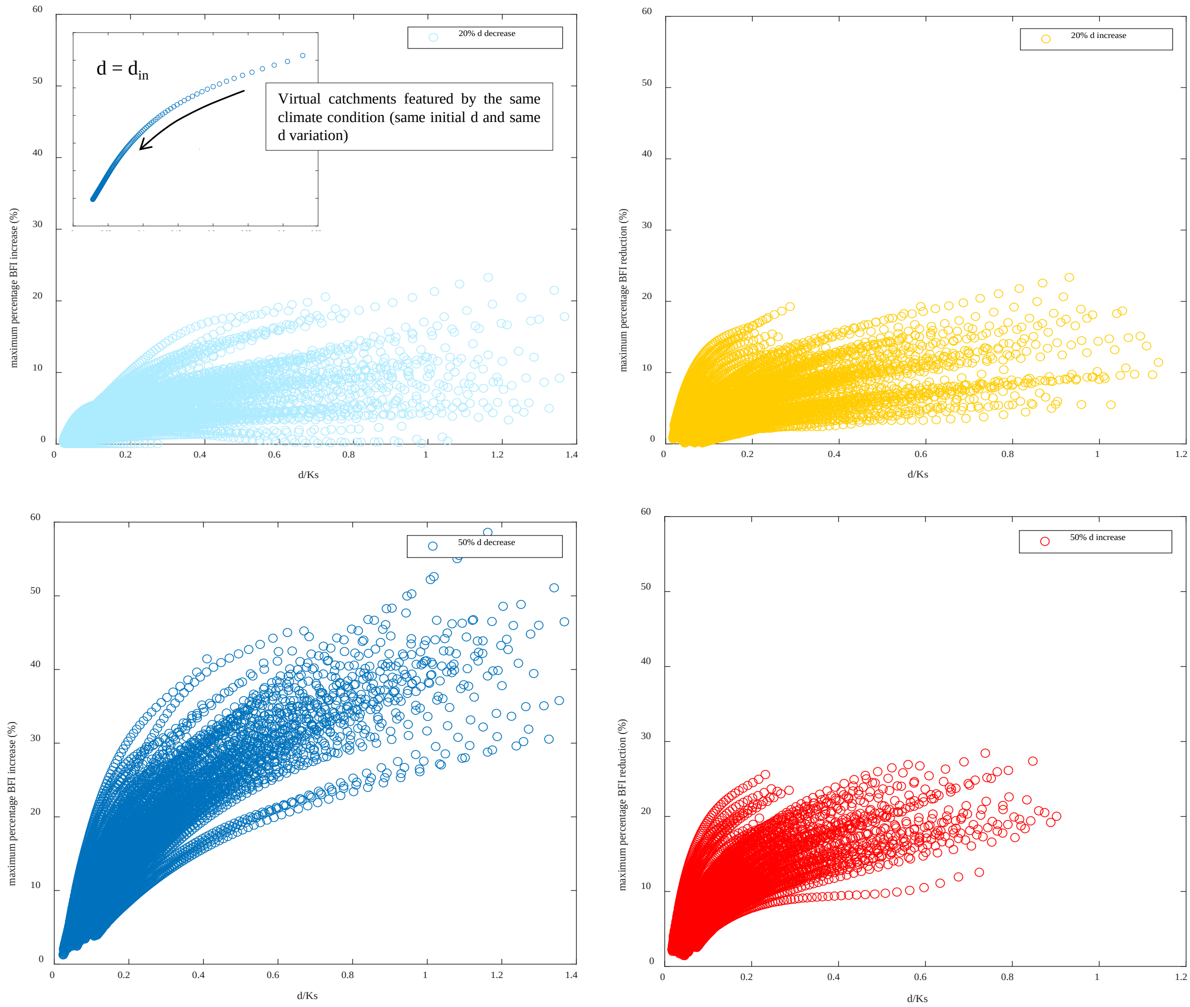

Figure 9. Maximum percentage BFI increase (left panels) and decrease (right panels) as a function of d/Ks. Light colours (upper panel) define 20% decrease or increase in d, dark colours (lower panel) define 50% decrease or increase in d.

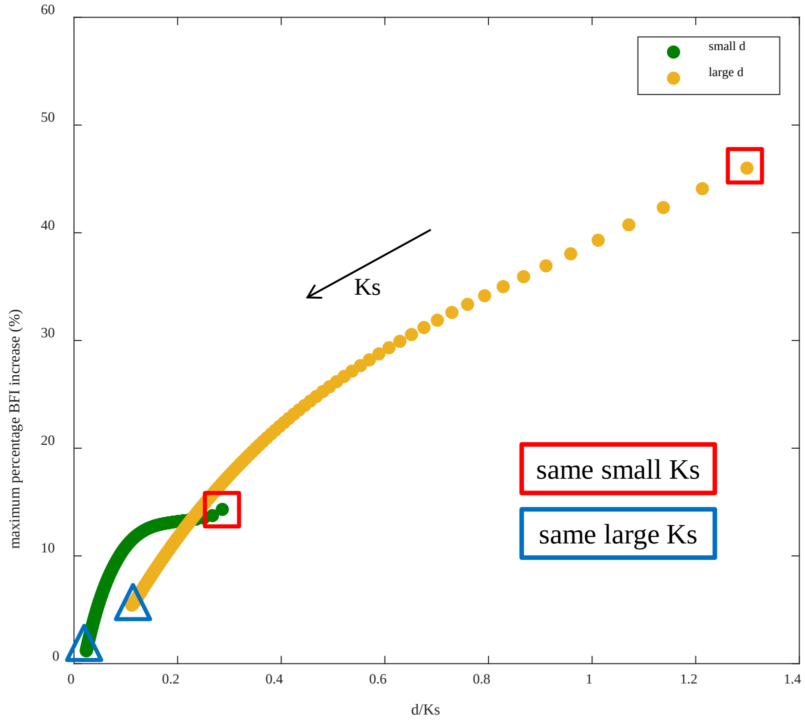

Figure 10. Modelled BFI variability induced by a decrease in d of 50% in the case of dry initial conditions (large d) and wet initial conditions (small d). Virtual catchments inside red and blue boxes are characterized by the same Ks value.

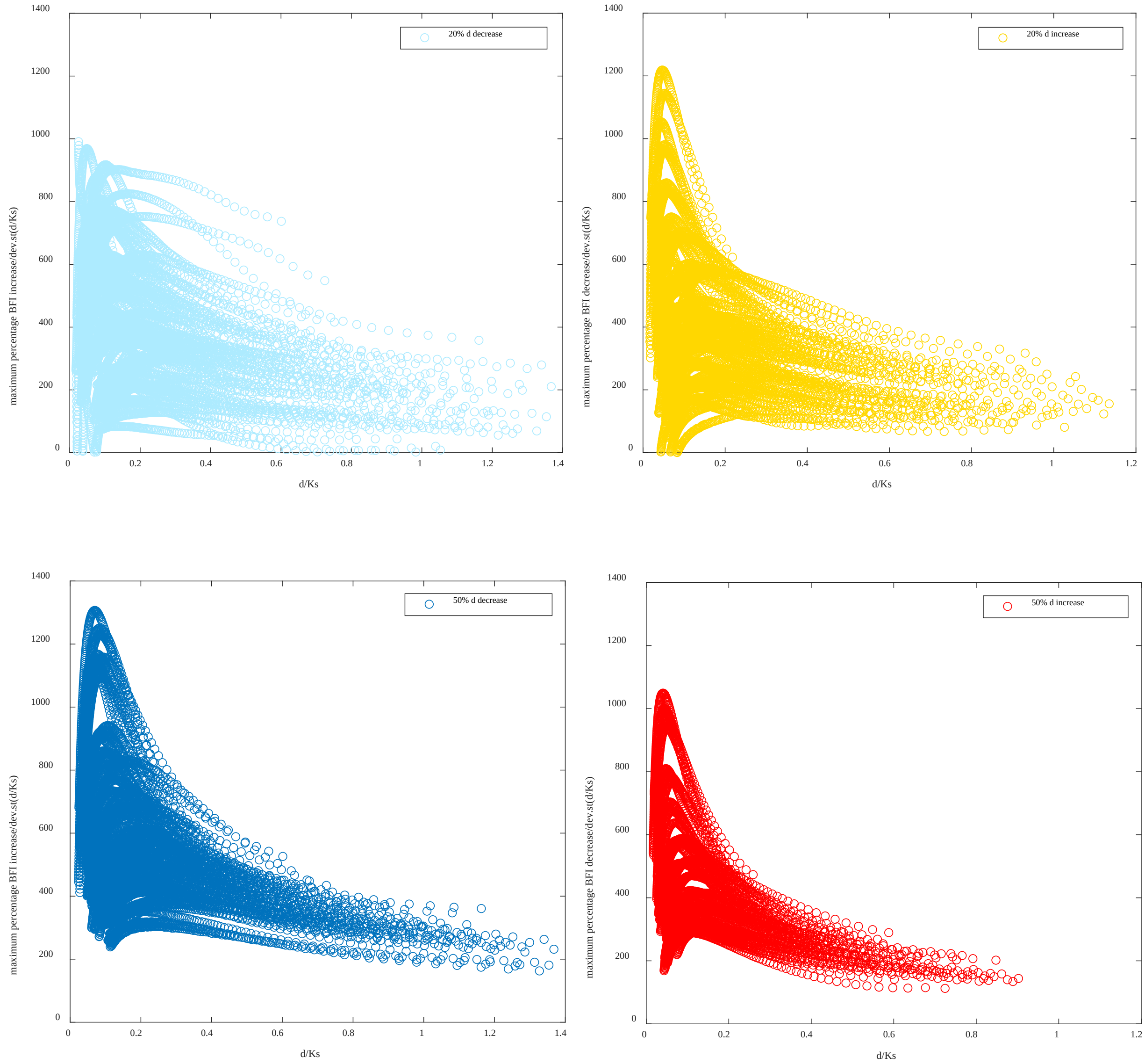

Figure 11. Ratio between BFI maximum percentage increase and decrease and d/Ks standard deviation for a decrease (left panels) and an increase (right panels) of the dry spell length d. Light colours (upper panel) define 20% decrease or increase in d; dark colours (lower panel) define 50% decrease or increase in d.

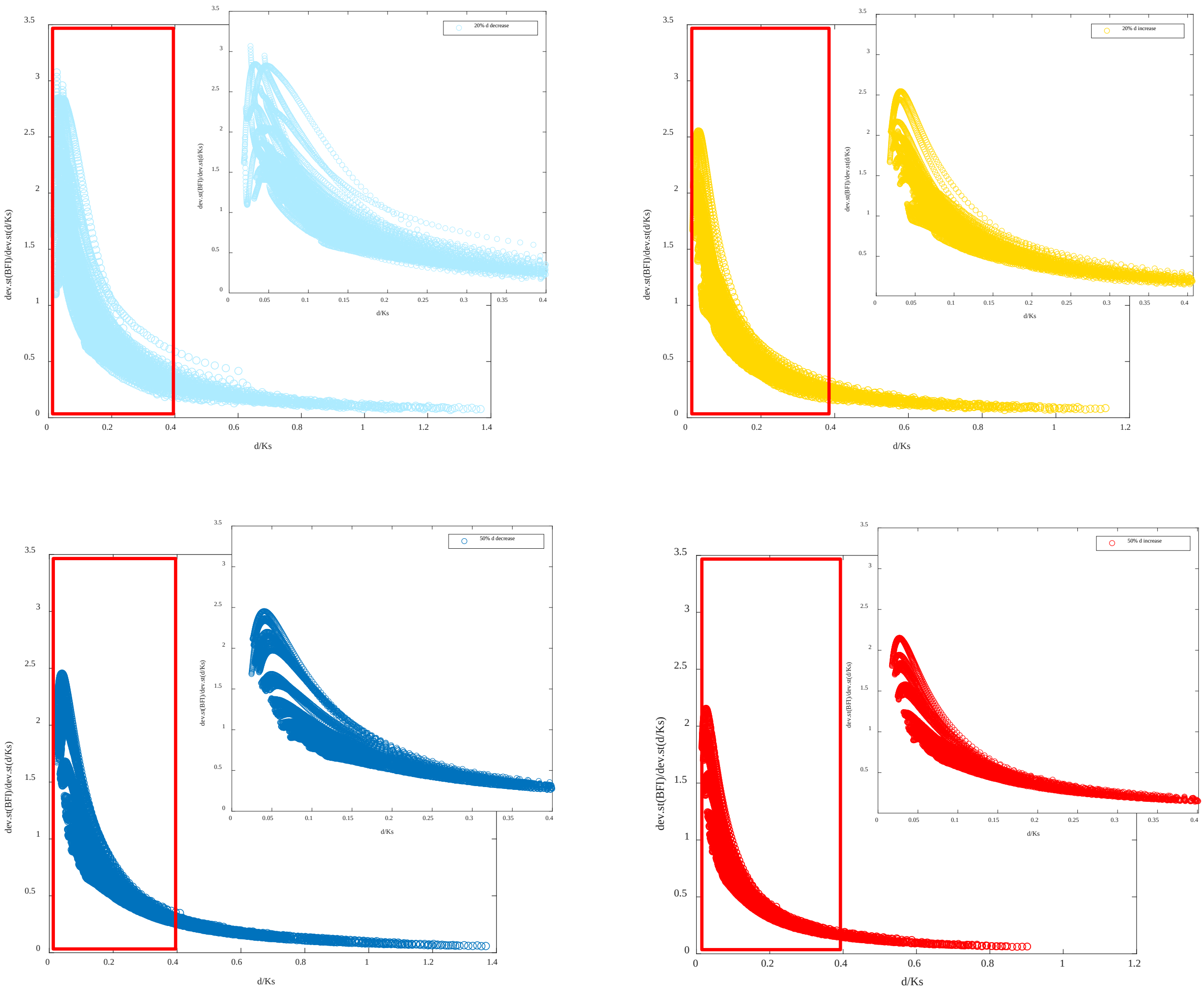

Figure 12. Ratio between BFI standard deviation and d/Ks standard deviation for a decrease (left panels) and an increase (right panels) of the dry spell length d. Light colours (upper panel) define 20% decrease or increase in d; dark colours (lower panel) define 50% decrease or increase in d. Plot areas included in the red boxes are enlarged in the adjacent illustrations.

Catchments	Cod	Latitude	Longitude	A (km^2)	Hmed (a.m.s.l.)	Climate	MAP (mm)	MAR (mm)	Permeability (m/s)	Soil type (FAO soil groups)	BFI
Hupsel	HUP	52.08	6.62	6.5	30	Cfb	654	270	10^{-9}	Podzols	0.35
Alento	ALE	42.43	14.09	270	328	Csa, Csb	1254	506	10^{-6}	Cambisols	0.3
Platis	PLA	35.10	24.69	210	698	Csa	930	241	10^{-8}	Leptosols	0.23
Calore	CAL	40.55	15.18	805	658	Csa, Csb	1362	859	10^{-5}	Cambisols	0.36
Djidiouia	DJE	35.97	0.88	835	468	Bsh	347	22	10^{-8}	Calcisols	0.25
Liri	LIR	41.72	13.62	480	1060	Csa, Csb	1445	978	10^{-7}	Cambisols	0.58
Noor	NOO	52.14	5.81	10.6	165	Cfb	869	164	10^{-4}	Podzols	0.86
Bussento Caselle	BUS	40.23	15.54	125	667	Csa, Csb	1588	1309	10^{-5}	Cambisols	0.76
Sele Albanella	SEL	40.48	15.10	3216	684	Csa, Csb	1210	545	10^{-6}	Cambisols	0.54
Guadiana	GUA	39.25	-3.75	16479	769	Csa, Bsh	452	37	10^{-8}	Calcisols	0.65

Table 1. Investigated catchments characteristics: assigned identification code (Cod), geographical coordinates (Latitude and Longitude), catchment drainage area (A), catchment mean elevation (Hmed), climate classes, according to Koppen climate classification (Climate), mean annual precipitation (MAP), mean annual runoff (MAR), permeability (Gleeson et al., 2014), soil type and baseflow index (BFI).

Catchments	Ks (days)	vs	NSE	R^2	LNSE	D	BFI_{cal}	BFI err(%)
Hupsel	30.2	0.21	0.74	0.88	0.64	0.66	0.39	-11.4
Alento	66.0	0.33	0.67	0.82	0.71	0.77	0.28	6.7
Platis	44.1	0.28	0.69	0.85	0.63	0.76	0.25	-8.7
Calore	60.0	0.43	0.72	0.85	0.68	0.75	0.39	-8.3
Djidiouia	40.0	0.30	0.72	0.86	0.70	0.83	0.24	4.0
Liri	102.0	0.53	0.73	0.85	0.74	0.76	0.57	1.7
Noor	202.9	0.93	0.74	0.86	0.77	0.80	0.92	-7.0
Bussento Caselle	122.7	0.81	0.67	0.81	0.45	0.63	0.64	3.0
Sele Albanella	80.0	0.55	0.72	0.85	0.73	0.74	0.50	7.4
Guadiana	120.0	0.49	0.71	0.85	0.68	0.73	0.62	4.6

Table 2. Model parameters and performances. Main reported model parameters are Ks (slow flow component delay time) and vs (slow flow component volumetric throughput coefficient). Used performance metrics are NSE (Nash-Sutcliff Efficiency coefficient), coefficient of determination (r2), LNSE (Nash-Sutcliffe Efficiency with logarithmic values) and D (index of agreement), BFI_{cal} (BFI derived by digital filtering of modelled time series), BFI err (percentage relative error between BFI and BFI_{cal}).

Catchments	mean obs (days)	max obs (days)	dev obs (days)	mean mod (days)	max mod (days)	dev mod (days)	AAPE (%)
Hupsel	3.18	19.00	2.86	2.70	18.00	2.18	3.65
Alento	7.72	47.00	6.19	5.79	50.00	4.08	-9.94
Platis	13.21	144.00	16.81	11.99	127.00	13.95	9.68
Calore	7.96	43.00	5.30	6.20	48.00	3.91	-14.91
Djidiouia	11.21	112.00	16.22	10.31	113.00	10.34	-1.43
Liri	7.54	42.00	5.03	6.20	51.00	3.87	-25.26
Noor	3.49	36.00	3.96	2.89	31.00	2.51	13.24
Bussento Caselle	7.95	66.00	6.63	5.94	62.00	3.98	4.92
Sele Albanella	9.49	29.00	3.51	6.80	30.00	2.05	-6.89
Guadiana	9.18	53.00	5.87	5.72	42.00	3.09	18.94

Table 3. Inter-storm durations: main descriptive statistics (mean, maximum and standard deviation values) for observed (obs) and modelled (mod) daily rainfall and average absolute percentage error (AAPE).

Catchments	mean obs (mm)	max obs (mm)	dev obs (mm)	mean mod (mm)	max mod (mm)	dev mod (mm)	AAPE (%)
Hupsel	1.83	33.10	3.59	1.47	41.13	3.11	-26.57
Alento	3.53	77.50	8.23	2.80	89.65	7.22	-17.35
Platis	2.55	95.40	7.31	1.95	69.41	4.90	27.36
Calore	3.30	65.80	6.47	2.38	68.47	5.46	-5.66
Djidiouia	0.98	61.80	3.81	0.81	69.58	3.28	-13.01
Liri	3.98	125.00	8.94	2.88	94.17	6.82	24.59
Noor	2.39	72.00	4.90	1.65	42.52	3.53	41.34
Bussento Caselle	4.36	137.00	11.53	3.34	109.08	8.54	20.33
Sele Albanella	3.32	50.70	6.01	2.25	62.21	4.44	-26.37
Guadiana	1.24	49.60	2.94	1.74	46.77	3.82	7.00

Table 4. Rainfall intensity: main descriptive statistics (mean, maximum and standard deviation values) for observed (obs) and modelled (mod) daily rainfall and average absolute percentage error (AAPE).

	vs	Ks (days)	d (days)
min value	0.1	15	3
max value	0.9	250	20

Table 5. Range of the main models parameters used in the virtual catchments simulation.